AGU PUBLICATIONS

Geophysical Research Letters

RESEARCH LETTER

10.1002/2014GL059923

Key Points:
- The impact of Antarctic Bottom Water warming is studied with an ocean model
- The simulated abyssal warming trend is congruent with observational evidence
- The abyssal warming enhances the Atlantic meridional overturning circulation

Supporting Information:
- Readme
- Figure S1
- Figure S2
- Figure S3
- Figure S4

Correspondence to:
L. Patara,
lpatara@geomar.de

Citation:
Patara, L., and C. W. Böning (2014), Abyssal ocean warming around Antarctica strengthens the Atlantic overturning circulation, *Geophys. Res. Lett.*, *41*, doi:10.1002/2014GL059923.

Received 14 MAR 2014
Accepted 15 MAY 2014
Accepted article online 20 MAY 2014

Abyssal ocean warming around Antarctica strengthens the Atlantic overturning circulation

Lavinia Patara[1] and Claus W. Böning[1]

[1]GEOMAR Helmholtz Centre for Ocean Research Kiel, Kiel, Germany

Abstract The abyssal warming around Antarctica is one of the most prominent multidecadal signals of change in the global ocean. Here we investigate its dynamical impacts on the Atlantic Meridional Overturning Circulation (AMOC) by performing a set of experiments with the ocean-sea ice model NEMO-LIM2 at ½° horizontal resolution. The simulations suggest that the ongoing warming of Antarctic Bottom Water (AABW), already affecting much of the Southern Hemisphere with a rate of up to 0.05°C decade^{-1}, has important implications for the large-scale meridional overturning circulation in the Atlantic Ocean. While the abyssal northward flow of AABW is weakening, we find the upper AMOC cell to progressively strengthen by 5–10% in response to deep density changes in the South Atlantic. The simulations suggest that the AABW-induced strengthening of the AMOC is already extending into the subtropical North Atlantic, implying that the process may counteract the projected decrease of the AMOC in the next decades.

1. Introduction

In the seas around Antarctica, intense ocean heat loss and brine formation create the densest water mass in the global ocean. Antarctic Bottom Water (AABW) sinks into the abyss and remains relatively isolated from further heat exchanges as it spreads northward to fill the deepest ocean with frigid dense waters [*Orsi et al.*, 1999]. Recent temperature analyses of repeat hydrographic sections reveal a nearly global signature of warming in the abyssal open ocean [*Purkey and Johnson*, 2010; *Kouketsu et al.*, 2011; *Azaneu et al.*, 2013] and a sustained loss of waters colder than 0°C since the 1980s [*Purkey and Johnson*, 2012]. Abyssal warming is most intense close to the source regions of AABW in the Southern Ocean from where it extends northward into all three major oceans [*Fukasawa et al.*, 2004; *Zenk and Morozov*, 2007; *Purkey and Johnson*, 2010; *Zenk and Visbeck*, 2013].

The warming of AABW represents a prominent signal of change in Earth's climate, yet its causes are still under investigation. One possibility is a reduction of AABW formation, associated with a slowdown of the bottom limb of the meridional overturning circulation [*Johnson et al.*, 2008; *Purkey and Johnson*, 2012]. An overall reduction of AABW formation rates is consistent with the concomitant freshening of dense shelf waters observed along the Antarctic coast [*Jacobs et al.*, 2002; *Aoki et al.*, 2013; *van Wijk and Rintoul*, 2014], possibly associated with an accelerated disintegration of ice sheets [*Jacobs et al.*, 2002] and an enhancement of the hydrological cycle [*Aoki et al.*, 2013]. An alternative hypothesis relates the abyssal warming in the Atlantic to variable wind-forced export of bottom waters [*Meredith et al.*, 2011]. In particular, the recent intensification of the Weddell Gyre may have progressively restricted the coldest AABW waters from crossing the South Scotia Ridge [*Meredith et al.*, 2008]. Both a reduced formation rate of AABW and the intensification of the Weddell Gyre may be regarded as consequences of the positive trend in the Southern Hemisphere westerly winds [*Marshall*, 2003]. Since the strengthening of westerly winds is projected to continue under rising greenhouse gas emissions [*Gillett and Fyfe*, 2013], it is plausible that the warming trend of AABW will extend also in the next century [*Meehl et al.*, 2011].

The consequences of AABW warming on the global climate are as yet uncertain. It is suggested that the AABW warming may have ramifications for global energy budgets [*Meehl et al.*, 2011] and for the rate of sea level rise [*Seidov et al.*, 2001; *Domingues et al.*, 2008; *Purkey and Johnson*, 2013]. Changes in Southern Ocean density are also thought to affect the strength of the Atlantic Meridional Overturning Circulation (AMOC), comprising the northward flow of warm, buoyant waters in the upper layer of the South and North Atlantic Ocean, its compensation by the southward flow of North Atlantic Deep Water (NADW) between

approximately 1000 and 4000 m depth, and northward flow of AABW below [*Lozier*, 2010]. Several modeling studies suggest a multidecadal to multicentennial seesaw relationship between deep water formation in the North and South Atlantic, triggered by changes in melting of ice sheets and sea ice [*Seidov et al.*, 2001; *Swingedouw et al.*, 2009; *Martin et al.*, 2014] and by modifications in deep ocean densities in the South Atlantic [*Kamenkovich and Goodman*, 2000; *Kamenkovich and Radko*, 2011].

Based on these studies, it can be hypothesized that the observed warming of AABW might affect the strength of the AMOC, thereby possibly acting as a driver of North Atlantic climate variation. Whether the ongoing AABW warming can generate a dynamical response on the AMOC, and with which amplitude and time scales, is, however, still unknown and is the topic of this study. To this end we perform a set of global ocean simulations designed to isolate the response of the AMOC to the observed warming trend of abyssal waters around Antarctica.

2. Methods

The simulations are carried out with a global configuration of the ocean general circulation model including sea ice NEMO-LIM2 [*Madec*, 2008] employing a nominal 0.5° horizontal resolution (ORCA05) and 46 unequally spaced levels. Its state-of-the-art configuration has been developed by the DRAKKAR collaboration [*DRAKKAR Group*, 2007] and was used in a wide range of applications [*Biastoch et al.*, 2008; *Schwarzkopf and Böning*, 2011; *Behrens et al.*, 2012]. The ocean model is forced by bulk formulae using a "normal" year forcing, i.e., a repeated annual cycle of wind and thermohaline surface fields obtained from atmospheric reanalysis products and satellite observations [*Large and Yeager*, 2009]. The simulations are initialized with temperature and salinity from the World Ocean Atlas [*Levitus et al.*, 1998] and integrated for 90 years.

The experiments are designed to isolate the effects of the recent AABW warming on the AMOC. It should be stressed here that our aim is not to investigate the causes of the abyssal warming trend, but its consequences. Our strategy is therefore to compare two identical model solutions differing only for the warming trend of the recently formed AABW. The control experiment (CTRL) is constrained to exhibit virtually constant AABW properties in time (Figure S1 in the supporting information), whereas the sensitivity experiment (WARM) exhibits a warming trend of AABW close to observed; the warming trend corresponds to a "contraction" of AABW, since its definition is based on a fixed density criterion as in previous studies [*Purkey and Johnson*, 2012; *Azaneu et al.*, 2013]. The AABW warming trend is achieved by using a standard configuration of ORCA05 exhibiting very little formation of AABW on the continental shelf, as typical for this class of ocean models [*Goosse et al.*, 2001; *Heuzé et al.*, 2013]. The WARM experiment therefore naturally simulates the observed trend of AABW warming and volume loss without a need to impose external constraints. For the CTRL experiment we apply a three-dimensional relaxation sponge in areas of recently formed AABW (black regions outlined in Figure 1) where we relax temperature and salinity to the World Ocean Atlas climatology [*Levitus et al.*, 1998] with a time scale of 1 year. The sponge region is confined to water masses approximately south of the 0.5°C isotherm, defining the Southern Antarctic Circumpolar Current Front. In the vertical, the sponge is restricted to a depth below 1000 m, where the largest deep warming trends have been observed in the Southern Ocean [*Purkey and Johnson*, 2010; *Kouketsu et al.*, 2011], and 500 m above the ocean bottom in order to avoid spurious sources of vorticity. We remark that while in reality the warming is highest in the deepest reaches of the Southern Ocean, the lack of relaxation close to the bottom would not alter our results since the coldest classes of AABW cannot escape the Weddell Sea and Ross Sea directly.

We analyze the effects of the multidecadal AABW warming around Antarctica by focusing on the evolution of the differences between the WARM and CTRL experiments (hereafter called DIFF). It should be emphasized that, since the CTRL and WARM experiments differ only for the AABW property trends around Antarctica, any other (spurious) trend unrelated to the impacts of AABW warming will cancel by analyzing the difference between the two simulations.

3. Results

The prime signal exhibited by the DIFF solution is the progressive spreading of the abyssal warming from the source regions around Antarctica over the entire Southern Hemisphere (Figure 1 and S2).

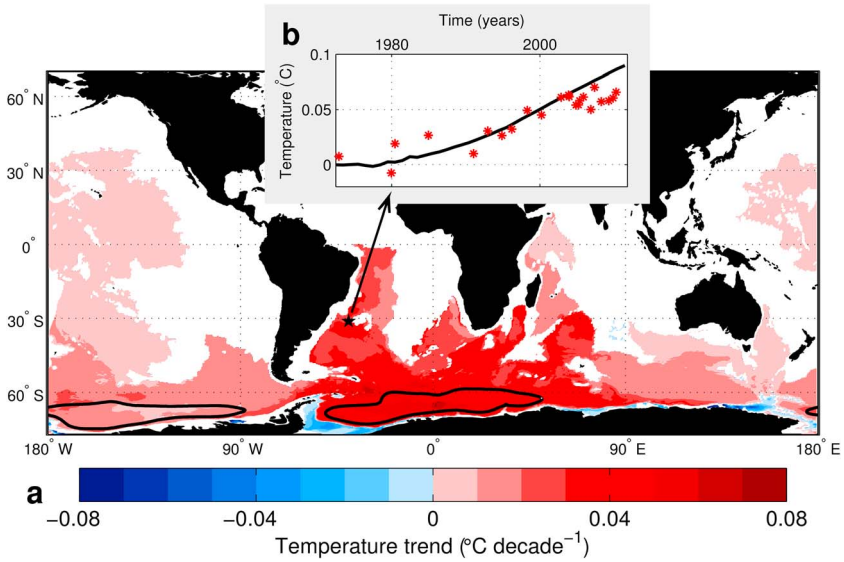

Figure 1. (a) Linear potential temperature trend from year 21 to 90 of DIFF computed over the AABW depth range, defined as depths for which potential density referenced to 4000 m (σ_4) is higher than 1045.91 kg m^{-3} (grey full contour in Figure 2). Values lower than 0.001°C decade^{-1} are not shown. Black contours show areas of prescribed AABW properties below 1000 m depth. (b) Simulated and observed potential temperature anomalies in the Vema Channel (star in Figure 1a); black line: annual mean temperature averaged below 2900 m depth in DIFF; red asterisks: observed bottom temperature anomalies [*Zenk and Visbeck*, 2013]. Anomalies are computed by subtracting the time series by the temperature values averaged over the first decade. The time axis refers to the observational time series, where we allocate year 1 of the model simulation to the first year of the observed time series (i.e., 1972).

The linear temperature trend in the AABW depth range, selected using a density criterion (grey full contour in Figure 2), is maximum in the South Atlantic sector, with values exceeding 0.05°C decade^{-1}. From there the signal spreads around the Southern Ocean and invades all ocean basins with patterns and magnitudes similar to those conjectured from the sparse observational evidence [*Zenk and Morozov*, 2007; *Purkey and Johnson*, 2010; *Azaneu et al.*, 2013]. The northward spreading of the abyssal warming appears most pronounced in the western ocean basins, especially in the South Atlantic

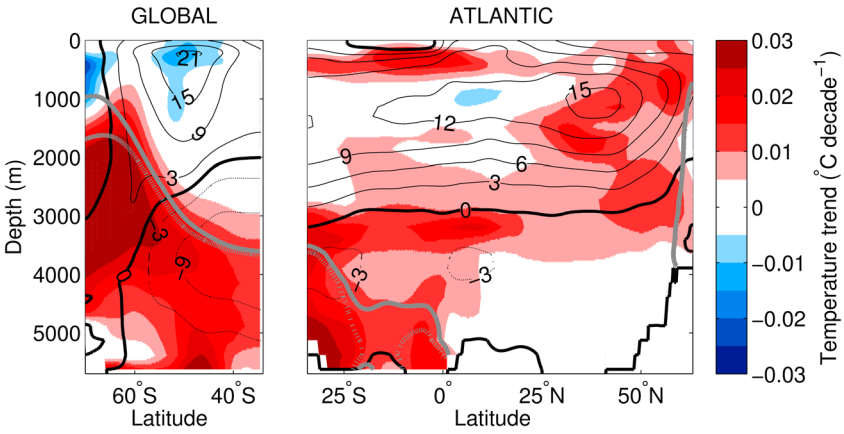

Figure 2. Colors: linear trend of zonally averaged potential temperature computed between the third and ninth decade of DIFF. (left) Zonal average over the globe; (right) zonal average over the Atlantic basin. Black contours: global (left) and Atlantic (right) meridional overturning circulation (Sv) averaged over years 21 to 90 of the CTRL experiment; positive (negative) values indicate clockwise (counterclockwise) circulation. Grey full contour: global (left) and Atlantic (right) zonal average of the 1045.91 kg m^{-3} potential density surface referenced to 4000 m depth (σ_4) averaged over years 21 to 90 of the CTRL experiment; grey dashed contour: same but for the last two decades of the WARM experiment. Smoothing has been applied to enhance visual clarity.

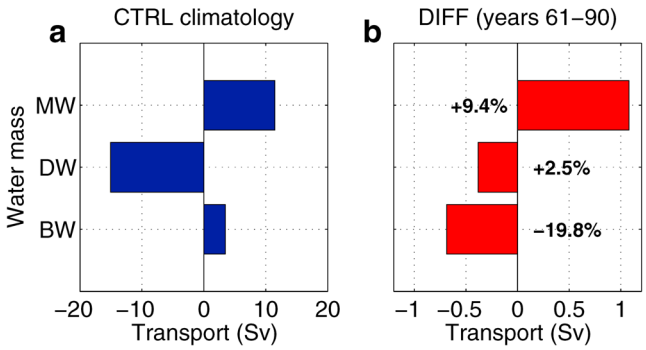

Figure 3. Atlantic meridional transport at 30°S for different density classes, where MW indicates northward flow of mode and intermediate waters, DW indicates southward flow of NADW, and BW indicates northward flow of AABW. The density classes have been computed separately for each experiment based on average profiles of potential density and meridional velocities. Potential density referenced at 2000 m has been used for the boundary between MW and DW, while potential density referenced at 4000 m has been used for the boundary between DW and BW. (a) Climatology over years 21 to 90 of the CTRL experiment. (b) Average over the last three decades of DIFF (i.e., WARM minus CTRL). Percentage changes with respect to the CTRL climatology are also shown.

(Figure 1). In the western Indian and Pacific Oceans the rates are somewhat weaker but extend farther into the Northern Hemisphere. Along its path in the western Atlantic, AABW flowing through the Vema Channel (depicted by the star in Figure 1a) warms by 0.02–0.03°C decade^{-1} comparable to the observed trend of about 0.02°C decade^{-1} since the 1980s [*Zenk and Morozov*, 2007; *Zenk and Visbeck*, 2013] shown as red stars in Figure 1b. The AABW layer in DIFF is contracting by 5–10 m yr^{-1} in the Southern Ocean (Figure S3), in agreement with observational accounts [*Purkey and Johnson*, 2012; *Azaneu et al.*, 2013].

The progression of the warming signal from the Antarctic seas into the ocean basins can partly be understood in terms of an advection by the mean abyssal flow, as manifested in a northward wedge of increasing temperatures broadly along the lower limb of the AABW-overturning cell (Figure 2). However, some aspects of the warming pattern cannot be reconciled by a purely advective spreading. One intriguing aspect is the rapid onset of the quasi-linear warming trend in the Vema Channel (Figure 1b), which cannot be explained by advection by the weak abyssal velocities, typically in the order of 0.1 to 1 cm s^{-1}. The rapid northward propagation along the South American coast is rather indicative of dynamical wave processes induced by the slumping of deep isotherms, as previously inferred for the Atlantic Ocean [*Swingedouw et al.*, 2009] and for the Pacific Ocean [*Masuda et al.*, 2010].

Since the progressive AABW warming is primarily confined to the western basins of the South Atlantic (Figure 1), it leads to modifications of deep zonal density gradients (Figure S4) and, through the thermal wind relation, to changes in the vertical shear of meridional velocities. We quantify this effect by computing the changes in meridional volume transport in the different density classes of water masses flowing at 30°S (Figure 3). Our results show that—over a period of 75 years—AABW northward transport decreases by 20%, NADW southward transport increases by 3%, and the northward transport of mode and intermediate waters increases by 9%. This pattern of change of the meridional transport reflects a progressive weakening of the lower limb of the AMOC, consistent with observed budget estimations in the North Atlantic [*Johnson et al.*, 2008], and a strengthening and downward expansion of the upper AMOC cell (Figure 4a), concurrent with a temperature increase at the transition between the upper and lower AMOC cells (Figure 2). First occurring in the southern reaches of the Atlantic basin after about 20 years from the onset of the AABW warming, the AMOC response signal rapidly extends to the equator within a few years, followed by a more gradual northward progression over the whole extent of the North Atlantic on a decadal time scale (Figure 4b). The propagation characteristics are consistent with idealized model studies [*Kawase*, 1987; *Goodman*, 2001; *Johnson and Marshall*, 2002] and reconstructed behavior in the North Pacific [*Masuda et al.*, 2010], involving a fast signal transmission by Kelvin waves along the western boundary to the equator, eastward along the equator, followed by a slower adjustment through Rossby waves radiating from the eastern boundary.

The idealized time line of DIFF can be translated into a figure tangible for the real world by associating the observed onset of the warming in the Vema Channel (i.e., the 1980s, Figure 1b) with the onset of the warming in DIFF (i.e., the second decade of simulation, Figure 1b). With this time allocation, the current state of the AMOC response would be represented by the fifth decade of the model simulation (highlighted between black contours in Figure 4b). At this stage the response of the

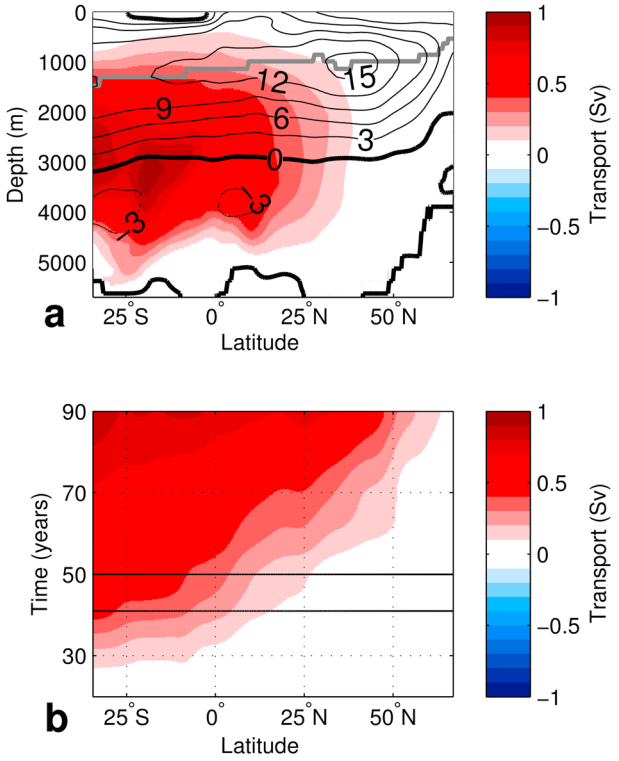

Figure 4. (a) Contours: Mean AMOC averaged over years 21 to 90 of the CTRL experiment. Colors: AMOC averaged over the fifth decade (years 41 to 50) of DIFF. The grey line indicates the depth of the maximum AMOC plotted in Figure 4b. We remark that the depth of the maximum AMOC is very similar for the CTRL and WARM experiments. (b) Temporal evolution of the annually averaged AMOC maximum in DIFF. The black lines indicate the fifth decade of DIFF which, according to our assumed time allocation (see text), corresponds to the decade in which we are currently in (i.e., 2010s). Smoothing has been applied to enhance visual clarity.

upper AMOC cell has clearly invaded the North Atlantic with a continuous trend of about 0.2 Sverdrup (Sv) decade^{-1}. According to the model results, the abyssal warming trend around Antarctica should thus have begun to affect the multidecadal evolution of the AMOC in the subtropical North Atlantic. It should be emphasized that although the simulated changes in the upper AMOC cell triggered by AABW warming are small compared to the intraseasonal and year-to-year AMOC variability, which amounts to about 20% of the mean [*Cunningham et al.*, 2007], it is their sustained nature and large meridional extent that could make them a relevant signal for the North Atlantic heat budget over the course of the 21st century. Indeed, paleoclimate reconstructions as well as climate simulations have shown that AMOC anomalies of this order of magnitude are associated with sea surface temperature anomalies capable of significantly affecting North Atlantic climate on multidecadal time scales [*Knight et al.*, 2005; *Park and Latif*, 2008; *Delworth and Zeng*, 2012].

4. Summary and Discussion

In this study we investigated the dynamical impact of the ongoing multidecadal abyssal warming around Antarctica onto the North Atlantic MOC. The simulated AABW warming trend, affecting much of the Southern Hemisphere with a rate of up to 0.05°C decade^{-1}, is congruent with the observational evidence. Following the main pathway of the newly formed AABW, the abyssal warming is mostly confined to the western South Atlantic where it causes a change in the east-west density gradients and in the vertical shear of meridional velocities. Our simulations suggest that while the AABW transport is weakening, the upper cell of the AMOC progressively strengthens. This response is consistent with a seesaw behavior between deep water formation in the North and South Atlantic, already detected in a multicentennial context in response to freshwater perturbations [*Seidov et al.*, 2001; *Swingedouw et al.*, 2007; *Martin et al.*, 2014]. By isolating the dynamical impact of the ongoing abyssal warming around Antarctica, we showed that the AABW-induced strengthening of the upper AMOC cell is already extending into the subtropical North Atlantic and that if continuing over the next decades, it will become a factor of multidecadal change rivaling or exceeding the weak multidecadal signal inferred for the last century [*Knight et al.*, 2005].

Due to the linkage of multidecadal changes in AMOC strength with North Atlantic climate conditions [*Gulev et al.*, 2013] it is imperative to gain a better understanding of drivers of AMOC multidecadal trends under increasing anthropogenic pressure. Climate model simulations in support of the fifth Coupled Model Intercomparison Project (CMIP5) predict a weakening of the upper limb of the AMOC by 20%–40% during the 21st century [*Weaver et al.*, 2012] as a result of dwindling deep water formation in the subpolar North Atlantic. A potential mechanism that may counteract this tendency is an increased salinity injection into the upper limb of the AMOC due to strengthening of the Agulhas leakage [*Biastoch et al.*, 2008]. This study

identifies another stabilizing mechanism—by itself leading to a 5%–10% increase of the AMOC over the 21st century—associated with ocean climate trends around Antarctica, which could add to the impact of the increased upper layer inflow of salinity to partially offset AMOC trends in the North Atlantic. Since AABW warming as well as reduced deep water formation in the North Atlantic are thought to be two aspects of the anthropogenic greenhouse gas increase [*Meredith et al.*, 2008; *Meehl et al.*, 2011; *Weaver et al.*, 2012; *Gillett and Fyfe*, 2013], their superposition would lead to a more limited weakening of the upper AMOC cell in the next century.

It is important to emphasize that present modeling capabilities, including the most recent CMIP5 simulations [*Heuzé et al.*, 2013], are unlikely capable of simulating the correct AABW warming patterns in response to climate change. This is due to the lack in essential physical processes involved in AABW formation, which in most coupled climate models lead to too much AABW formation through open ocean convection in the Weddell Sea instead of on the continental shelf [*Heuzé et al.*, 2013; *Martin et al.,* 2014]. This causes an incorrect simulation of AABW water mass properties [*Goosse et al.*, 2001] and of its sensitivity to atmospheric forcing [*Gordon*, 1991]. Accordingly, our experimental strategy was not directed at discerning the causes responsible for the ongoing warming of AABW, but at isolating its consequences on the AMOC by prescribing the observed warming trend to the newly formed AABW. Nonetheless, our results point to the importance of including the explicit simulation of these processes into climate models, in order to achieve a more realistic response of the AMOC to anthropogenic climate change and to improve North Atlantic climate predictions on multidecadal time scales.

Acknowledgments

The model data used for this paper can be made available from the author upon request. The integration of the experiments has been performed at the Computing Centre of the Kiel University and at the North-German Supercomputing Alliance (HLRN). The study was financially supported by the Deutsche Forschungsgemeinschaft (DFG) project BO 907/4-1 and by the project CP1219 of the Cluster of Excellence "The Future Ocean" funded within the framework of the Excellence Initiative by the DFG. We thank Walter Zenk for providing the observed temperature data at the Vema Channel and the NEMO and DRAKKAR teams for their technical support. Two anonymous reviewers are also gratefully acknowledged.

The Editor thanks two anonymous reviewers for their assistance in evaluating this paper.

References

Aoki, S., Y. Kitade, K. Shimada, K. I. Ohshima, T. Tamura, C. C. Bajish, M. Moteki, and S. R. Rintoul (2013), Widespread freshening in the Seasonal Ice Zone near 140°E off the Adélie Land Coast, Antarctica, from 1994 to 2012, *J. Geophys. Res. Oceans*, *118*, 6046–6063, doi:10.1002/2013JC009009.

Azaneu, M., R. Kerr, M. M. Mata, and C. A. E. Garcia (2013), Trends in the deep Southern Ocean (1958–2010): Implications for Antarctic Bottom Water properties and volume export, *J. Geophys. Res. Oceans*, *118*, 4213–4227, doi:10.1002/jgrc.20303.

Behrens, E., F. U. Schwarzkopf, J. F. Lubbecke, and C. W. Böning (2012), Model simulations on the long-term dispersal of Cs-137 released into the Pacific Ocean off Fukushima, *Env. Res. Lett.*, *7*(3), doi:10.1088/1748-9326/7/3/034004.

Biastoch, A., C. W. Böning, and J. R. E. Lutjeharms (2008), Agulhas leakage dynamics affects decadal variability in Atlantic overturning circulation, *Nature*, *456*, 489–492.

Cunningham, S. A., et al. (2007), Temporal variability of the Atlantic Meridional Overturning Circulation at 26.5 degrees N, *Science*, *317*, 935–938.

Delworth, T. L., and F. Zeng (2012), Multicentennial variability of the Atlantic Meridional Overturning Circulation and its climatic influence in a 4000 year simulation of the GFDL CM2.1 climate model, *Geophys. Res. Lett.*, *39*, L13702, doi:10.1029/2012GL052107.

Domingues, C. M., J. A. Church, N. J. White, P. J. Gleckler, S. E. Wijffels, P. M. Barker, and J. R. Dunn (2008), Improved estimates of upper-ocean warming and multi-decadal sea-level rise, *Nature*, *453*, 1090–1093.

DRAKKAR Group (2007), Eddy-permitting ocean circulation hindcasts of past decades, *CLIVAR Exchanges*, *12*(3), 8–10, International CLIVAR Project Office, Southampton, U. K.

Fukasawa, M., H. Freeland, R. Perkin, T. Watanabe, H. Uchida, and A. Nishina (2004), Bottom water warming in the North Pacific Ocean, *Nature*, *427*, 825–827.

Gillett, N. P., and J. C. Fyfe (2013), Annular mode changes in the CMIP5 simulations, *Geophys. Res. Lett.*, *40*, 1189–1193, doi:10.1002/grl.50249.

Goodman, P. J. (2001), Thermohaline adjustment and advection in an OGCM, *J. Phys. Oceanogr.*, *31*(6), 1477–1497, doi:10.1175/1520-0485(2001)031<1477:TAAAIA>2.0.CO;2.

Goosse, H., J. M. Campin, and B. Tartinville (2001), The sources of Antarctic bottom water in a global ice ocean model, *Ocean Modell.*, *3*(1-2), 51–65.

Gordon, A. L. (1991), Two stable modes of Southern Ocean winter stratification, in *Deep Convection and Deep Water Formation in the Oceans*, *Elsevier Oceanogr. Ser.*, vol. 57, edited by P. C. Chu and J. C. Gascard, pp. 17–35, Elsevier, Amsterdam, Netherlands.

Gulev, S. K., M. Latif, N. Keenlyside, W. Park, and K. P. Koltermann (2013), North Atlantic Ocean control on surface heat flux on multidecadal timescales, *Nature*, *499*, 464–467.

Heuzé, C., K. J. Heywood, D. P. Stevens, and J. K. Ridley (2013), Southern Ocean bottom water characteristics in CMIP5 models, *Geophys. Res. Lett.*, *40*, 1409–1414, doi:10.1002/grl.50287.

Jacobs, S. S., C. F. Giulivi, and P. A. Mele (2002), Freshening of the Ross Sea during the late 20th century, *Science*, *297*, 386–389.

Johnson, H. L., and D. P. Marshall (2002), A theory for the surface Atlantic response to thermohaline variability, *J. Phys. Oceanogr.*, *32*, 1121–1132.

Johnson, G. C., S. G. Purkey, and J. M. Toole (2008), Reduced Antarctic Meridional Overturning Circulation reaches the North Atlantic Ocean, *Geophys. Res. Lett.*, *35*, L22601, doi:10.1029/2008GL035619.

Kamenkovich, I. V., and P. J. Goodman (2000), The dependence of AABW transport in the Atlantic on vertical diffusivity, *Geophys. Res. Lett.*, *27*(22), 3739–3742, doi:10.1029/2000GL011675.

Kamenkovich, I. V., and T. Radko (2011), Role of the Southern Ocean in setting the Atlantic stratification and meridional overturning circulation, *J. Mar. Res.*, *69*(2-3), 277–308.

Kawase, M. (1987), Establishment of deep ocean circulation driven by deep-water production, *J. Phys. Oceanogr.*, *17*, 2294–2317.

Knight, J. R., R. J. Allan, C. K. Folland, M. Vellinga, and M. E. Mann (2005), A signature of persistent natural thermohaline circulation cycles in observed climate, *Geophys. Res. Lett.*, *32*, L20708, doi:10.1029/2005GL024233.

Kouketsu, S., et al. (2011), Deep ocean heat content changes estimated from observation and reanalysis product and their influence on sea level change, *J. Geophys. Res.*, *116*, C03012, doi:10.1029/2010JC006464.
Large, W. G., and S. G. Yeager (2009), The global climatology of an interannually varying air-sea flux data set, *Clim. Dyn.*, *33*, doi:10.1007/s00382-008-0441-3.
Levitus, S., et al. (1998), World ocean database 1998, vol. 1, Introduction, NOAA Atlas NESDIS, 18, NOAA, Silver Spring, Md.
Lozier, M. S. (2010), Deconstructing the Conveyor Belt, *Science*, *328*, 1507–1511.
Marshall, G. J. (2003), Trends in the southern annular mode from observations and reanalyses, *J. Clim.*, *16*, 4134–4143.
Madec, G. (2008), NEMO ocean engine, Note du Pole de modélisation, Institut Pierre-Simon Laplace (IPSL), France, No 27 ISSN No 1288-1619.
Martin, T., W. Park, and M. Latif (2014), Southern Ocean forcing of the North Atlantic at multi-centennial time scales in the Kiel Climate Model, *Deep Sea Res., Part II*, doi:10.1016/j.dsr2.2014.01.018.
Masuda, S., et al. (2010), Simulated rapid warming of abyssal north pacific waters, *Science*, *329*, 319–322.
Meehl, G. A., J. M. Arblaster, J. T. Fasullo, A. X. Hu, and K. E. Trenberth (2011), Model-based evidence of deep-ocean heat uptake during surface-temperature hiatus periods, *Nat. Clim. Change*, *1*, 360–364.
Meredith, M. P., A. C. N. Garabato, A. L. Gordon, and G. C. Johnson (2008), Evolution of the deep and bottom waters of the Scotia Sea, Southern Ocean, during 1995–2005, *J. Clim.*, *21*, 3327–3343.
Meredith, M. P., A. L. Gordon, A. C. Naveira Garabato, E. P. Abrahamsen, B. A. Huber, L. Jullion, and H. J. Venables (2011), Synchronous intensification and warming of Antarctic Bottom Water outflow from the Weddell Gyre, *Geophys. Res. Lett.*, *38*, L03603, doi:10.1029/2010GL046265.
Orsi, A. H., G. C. Johnson, and J. L. Bullister (1999), Circulation, mixing, and production of Antarctic Bottom Water, *Prog. Oceanogr.*, *43*, 55–109.
Park, W., and M. Latif (2008), Multidecadal and multicentennial variability of the meridional overturning circulation, *Geophys. Res. Lett.*, *35*, L22703, doi:10.1029/2008GL035779.
Purkey, S. G., and G. C. Johnson (2010), Warming of global abyssal and deep Southern Ocean waters between the 1990s and 2000s: Contributions to global heat and sea level rise budgets, *J. Clim.*, *23*, 6336–6351.
Purkey, S. G., and G. C. Johnson (2012), Global contraction of Antarctic Bottom Water between the 1980s and 2000s, *J. Clim.*, *25*, 5830–5844.
Purkey, S. G., and G. C. Johnson (2013), Antarctic Bottom Water warming and freshening: Contributions to sea level rise, ocean freshwater budgets, and global heat gain, *J. Clim.*, *26*, 6105–6122.
Schwarzkopf, F. U., and C. W. Böning (2011), Contribution of Pacific wind stress to multi-decadal variations in upper-ocean heat content and sea level in the tropical south Indian Ocean, *Geophys. Res. Lett.*, *38*, L12602, doi:10.1029/2011GL047651.
Seidov, D., E. Barron, and B. J. Haupt (2001), Meltwater and the global ocean conveyor: Northern versus southern connections, *Global Planet. Change*, *30*(3-4), 257–270, doi:10.1016/S0921-8181(00)00087-4.
Swingedouw, D., T. Fichefet, H. Goosse, and M. F. Loutre (2009), Impact of transient freshwater releases in the Southern Ocean on the AMOC and climate, *Clim. Dyn.*, *33*, 365–381.
van Wijk, E. M., and S. R. Rintoul (2014), Freshening drives contraction of Antarctic Bottom Water in the Australian Antarctic Basin, *Geophys. Res. Lett.*, *41*, 1657–1664, doi:10.1002/2013GL058921.
Weaver, A. J., et al. (2012), Stability of the Atlantic meridional overturning circulation: A model intercomparison, *Geophys. Res. Lett.*, *39*, L20709, doi:10.1029/2012GL053763.
Zenk, W., and E. Morozov (2007), Decadal warming of the coldest Antarctic Bottom Water flow through the Vema Channel, *Geophys. Res. Lett.*, *34*, L14607, doi:10.1029/2007GL030340.
Zenk, W., and M. Visbeck (2013), Structure and evolution of the abyssal jet in the Vema Channel of the South Atlantic, *Deep Sea Res., Part II*, *85*, 244–260.